Monthly Notices
of the
ROYAL ASTRONOMICAL SOCIETY

Mon. Not. R. Astron. Soc. **400,** 1911–1918 (2009) doi:10.1111/j.1365-2966.2009.15577.x

Journey to the $M_{\rm BH}$–σ relation: the fate of low-mass black holes in the Universe

Marta Volonteri[1]⋆ and Priyamvada Natarajan[2,3]

[1]*Department of Astronomy, University of Michigan, Ann Arbor, MI, USA*
[2]*Department of Astronomy, Yale University, PO Box 208101, New Haven, CT 06511-208101, USA*
[3]*Radcliffe Institute for Advanced Study, Harvard University, 10 Garden Street, Cambridge, MA 02138, USA*

Accepted 2009 August 19. Received 2009 July 9; in original form 2009 March 10

ABSTRACT

In this paper, we explore the establishment and evolution of the empirical correlation between black hole mass ($M_{\rm BH}$) and velocity dispersion (σ) with redshift. We trace the growth and accretion history of massive black holes (MBHs) starting from high-redshift seeds that are planted via physically motivated prescriptions. Two seeding models are explored in this work: 'light seeds', derived from Population III remnants, and 'heavy seeds', derived from direct gas collapse. Even though the seeds themselves do not satisfy the $M_{\rm BH}$–σ relation initially, we find that the relation can be established and maintained at all times if self-regulating accretion episodes are associated with major mergers. The massive end of the $M_{\rm BH}$–σ relation is established early, and lower mass MBHs migrate on to it as hierarchical merging proceeds. How MBHs migrate towards the relation depends critically on the seeding prescription. Light seeds initially lie well below the $M_{\rm BH}$–σ relation, and MBHs can grow via steady accretion episodes unhindered by self-regulation. In contrast, for the heavy seeding model, MBHs are initially over-massive compared to the empirical correlation, and the host haloes assemble prior to kick-starting the growth of the MBH. We find that the existence of the $M_{\rm BH}$–σ correlation is purely a reflection of the merging hierarchy of massive dark matter haloes. The slope and scatter of the relation however appear to be a consequence of the seeding mechanism and the self-regulation prescription. We expect flux limited active galactic nucleus surveys to select MBHs that have already migrated on to the $M_{\rm BH}$–σ relation. Similarly, the Laser Interferometer Space Antenna (LISA) is also likely to be biased towards detecting merging MBHs that preferentially inhabit the $M_{\rm BH}$–σ. These results are a consequence of major mergers being more common at high redshift for the most massive, biased, galaxies that host MBHs which have already migrated on to the $M_{\rm BH}$–σ relation. We also predict the existence of a large population of low-mass 'hidden' MBHs at high redshift which can easily escape detection. Additionally, we find that if MBH seeds are massive, $\sim 10^5$ M$_\odot$, the low-mass end of the $M_{\rm BH}$–σ flattens towards an asymptotic value, creating a characteristic 'plume'.

Key words: accretion, accretion discs – black hole physics – hydrodynamics – instabilities – galaxies: formation – cosmology: theory.

1 INTRODUCTION

The demography of local galaxies suggests the that almost every galaxy hosts a quiescent super-massive black hole (MBH) at the present time and the properties of the MBH are correlated with those of the host. In particular, recent observational evidence points to the existence of a strong correlation between the mass of the central MBH and the velocity dispersion of the host spheroid (Ferrarese & Merritt 2000; Gebhardt et al. 2000; Tremaine et al. 2002; Marconi & Hunt 2003; Häring & Rix 2004; Gültekin et al. 2009) and possibly the host halo (Ferrarese 2002) in nearby galaxies. It is currently unclear if these correlations hold at higher redshift, or if the scalings evolve with cosmic time. These correlations strongly suggest coeval growth of the MBH and the stellar component via likely regulation of the gas supply in galactic nuclei (Silk & Rees 1998; Kauffmann & Haehnelt 2000; Fabian 2001; King 2003; Thompson, Quataert & Murray 2005; Natarajan & Treister 2009).

The current phenomenological approach to understand the assembly of MBHs involves data from both high and low

⋆E-mail: martav@umich.edu

redshifts. These data are used to construct a consistent picture that is in consonance with the larger framework of the growth and evolution of structure in the Universe (e.g. Haehnelt, Natarajan & Rees 1998; Haiman & Loeb 1998; Kauffmann & Haehnelt 2000; Kauffmann & Haehnelt 2002; Wyithe & Loeb 2002; Volonteri, Haardt & Madau 2003; Di Matteo, Springel & Hernquist 2005; Steed & Weinberg 2004). Major mergers appear to drive the establishment of the correlations between MBH masses and their host properties (Robertson et al. 2006; Peng 2007; Hopkins et al. 2007a,b) and it also appears that these correlations are possibly linear projections of a more universal MBH Fundamental Plane relation (Hopkins et al. 2007a). The observed correlations offer insight into how the dynamics of the merger process establish these relations.

In a companion paper (Volonteri, Lodato & Natarajan 2008), we explored the evolution of MBHs with cosmic history starting from physically motivated MBH formation models. We investigated the observational signatures by following the mass assembly of these black hole seeds to the present time. We showed that the low-redshift population evolved from physically motivated seeds agrees nicely with current constraints (mass function of MBHs at $z = 0$; the integrated mass density of black holes and the luminosity function of active galactic nucleus (AGN) as a function of redshift).

In this paper, we address the establishment of the correlation between MBH masses and the velocity dispersion of their host, by focusing on two relevant questions as we track the journey of black holes on to the observed $z = 0$ $M_{\rm BH}$–σ relation, (i) are the correlations established independently of galaxy mass, and (ii) can observations at $z > 0$ select samples unbiased with respect to the $M_{\rm BH}$–σ relation.

The structure of our paper is as follows. In the first and second sections, we outline very briefly the basic methodology adopted to track the merger history. In the third section, we focus on the details of the $M_{\rm BH}$–σ relation and its establishment with epoch and mass (in Section 4). The observational consequences of our model are described in Section 5 and our conclusions are discussed in the final section of this paper.

2 METHODOLOGY

We ground our models in the framework of the standard paradigm for the growth of structure in a Λ cold dark matter (ΛCDM) Universe – a model that has independent validation, most recently from *Wilkinson Microwave Anisotropy Probe (WMAP)* measurements of the anisotropies in the cosmic microwave background (Page et al. 2003; Spergel et al. 2003). Structure formation is tracked in cosmic time by keeping a census of the number of collapsed dark matter haloes of a given mass that form; these provide the sites for harbouring MBHs. The computation of the mass function of dark matter haloes is done using the extended Press–Schechter theory (Lacey & Cole 1993) and Monte Carlo realizations of merger trees (Volonteri et al. 2003). Monte Carlo merger trees are created for present-day haloes and propagated back in time to a redshift of $\sim$20. With the merging history thus determined, the haloes are then populated with seed MBHs. The halo merger sequence is followed and black holes are grown embedded in their dark matter halo.

2.1 The initial BH seeding model

We compare two distinct types of seeds: 'light seeds', derived from Population III remnants, and 'heavy seeds', where we plant the initial seeds in the dark matter haloes according to the prescription described in Volonteri et al. (2008) as per the physically motivated model developed by Lodato & Natarajan (2006, 2007).

In the 'heavy seeds' scenario, massive seeds with $M \approx 10^5$–$10^6\,{\rm M}_\odot$ can form at high redshift ($z > 15$), when the intergalactic medium has not been significantly enriched by metals (Koushiappas, Bullock & Dekel 2004; Begelman, Volonteri & Rees 2006; Lodato & Natarajan 2006, 2007). Here, we refer to Lodato & Natarajan (2006, 2007), for more details of the seeding model, wherein the development of non-axisymmetric spiral structures drives mass infall and accumulation in a pre-galactic disc with primordial composition. The mass accumulated in the centre of the halo (which provides an upper limit to the MBH seed mass) is given by

$$M_{\rm BH} = m_{\rm d} M_{\rm halo} \left[1 - \sqrt{\frac{8\lambda}{m_{\rm d} Q_{\rm c}} \left(\frac{j_{\rm d}}{m_{\rm d}}\right) \left(\frac{T_{\rm gas}}{T_{\rm vir}}\right)^{1/2}}\right], \quad (1)$$

for

$$\lambda < \lambda_{\rm max} = m_{\rm d} Q_{\rm c}/8(m_{\rm d}/j_{\rm d})(T_{\rm vir}/T_{\rm gas})^{1/2}, \quad (2)$$

and $M_{\rm BH} = 0$ otherwise. Here, $\lambda_{\rm max}$ is the maximum halo spin parameter for which the disc is gravitationally unstable, m_d is the gas fraction that participates in the infall and $Q_{\rm c}$ is the Toomre parameter. The efficiency of MBH formation is strongly dependent on the Toomre parameter $Q_{\rm c}$, which sets the frequency of formation, and consequently the number density of MBH seeds. Guided by our earlier investigation, we set $Q_{\rm c} = 2$ (the intermediate efficiency model) as described in Volonteri et al. (2008).

The efficiency of the seed assembly process ceases at large halo masses, where the disc undergoes fragmentation instead. This occurs when the virial temperature exceeds a critical value $T_{\rm max}$, given by

$$\frac{T_{\rm max}}{T_{\rm gas}} = \left[\frac{4\alpha_{\rm c}}{m_{\rm d}(1 + M_{\rm BH}/m_{\rm d}M_{\rm halo})}\right]^{2/3}, \quad (3)$$

where $\alpha_{\rm c} \approx 0.06$ is a dimensionless parameter measuring the critical gravitational torque above which the disc fragments (Rice, Lodato & Armitage 2005).

To summarize, every dark matter halo is characterized by its mass M (or virial temperature $T_{\rm vir}$) and by its spin parameter λ. The gas has a temperature $T_{\rm gas} = 5000\,{\rm K}$. If $\lambda < \lambda_{\rm max}$ (see equation 2) and $T_{\rm vir} < T_{\rm max}$ (equation 3), then we assume that a seed BH of mass $M_{\rm BH}$ given by equation (1) forms in the centre. The remaining relevant parameters are $m_{\rm d} = j_{\rm d} = 0.05$, $\alpha_{\rm c} = 0.06$ and here we consider the $Q_{\rm c} = 2$ case.

In the 'heavy seed' model, MBHs form (i) only in haloes within a narrow range of virial temperatures ($10^4\,{\rm K} < T_{\rm vir} < 1.4 \times 10^4\,{\rm K}$), hence, halo velocity dispersion ($\sigma \simeq 15\,{\rm km\,s^{-1}}$), and (ii) for each virial temperature all seed masses below $m_d M$ modulo the spin parameter of the halo are allowed (see equations 1 and 3). The seed mass function peaks at $10^5\,{\rm M}_\odot$, with a steep drop at $3 \times 10^6\,{\rm M}_\odot$. We refer the reader to Lodato & Natarajan (2007) and Volonteri et al. (2008) for a discussion of the mass function (and related plots). Here, we stress that given points (i) and (ii), the initial seeds do not satisfy the local $M_{\rm BH}$–σ relation, in fact the seed masses are not correlated with σ, as shown in the lower left-hand panels of Fig. 1 (see the almost vertical line in the $z = 4$ panels).

In the Population III remnants model ('light seeds'), MBHs form asend-product of the very first generation of stars, with masses $m_{\rm seed} \sim$ few $\times\, 10^2\,{\rm M}_\odot$. The first stars are believed to form at $z \sim 20$–30 in haloes which represent high-σ peaks of the primordial density

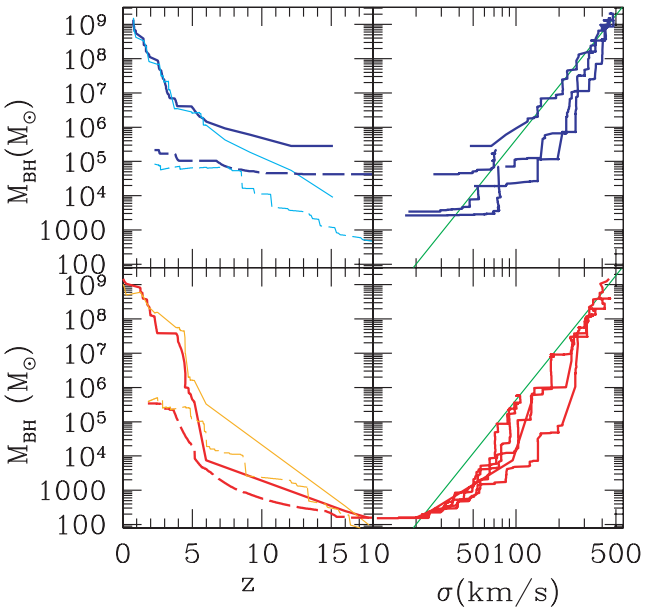

Figure 1. Tracks of MBH growth as a function of redshift or velocity dispersion along the history of a $4 \times 10^{13}\,M_\odot$ halo. Top: 'heavy seeds'; bottom: "light seeds". When we track the MBH growth as a function of redshift, we show with a solid curve the MBH in the main halo; with a dashed curve a MBH in a satellite galaxy. The thick lines show growth histories extracted from our models, the thin lines show the mass the MBH would have if it sat on the M_{BH}–σ relation at the times when we record MBH masses. If seeds are light, the MBHs typically have to catch up with their host, vice versa if seeds are heavy their growth is impeded if feedback effects that limit the MBH mass are at work.

field. The main coolant, in absence of metals, is molecular hydrogen, which is a rather inefficient coolant. The inefficient cooling might lead to a very top-heavy initial stellar mass function, and in particular to the production of an early generation of very massive stars (Carr, Bond & Arnett 1984). If stars form above $260\,M_\odot$, they would rapidly collapse to MBHs with little mass loss (Fryer, Woosley & Heger 2001), that is leaving behind seed MBHs with masses $M_{BH} \sim 10^2$–$10^3\,M_\odot$ (Madau & Rees 2001).

The main features of a scenario for the hierarchical assembly of MBHs left over by the first stars in a ΛCDM cosmology have been discussed by Volonteri et al. (2003) and Volonteri & Rees (2006). Stars, and their remnant MBHs, form in isolation within minihaloes above the cosmological Jeans mass collapsing at $z \geqslant 20$ from rare $\nu - \sigma$ peaks of the primordial density field (Madau & Rees 2001). We here consider $\nu = 3.5$, that is, very rare peaks of the primordial density field (Volonteri et al. 2003). We assume that seeds form in the mass range $125 < M_{BH} < 1000\,M_\odot$, from an initial stellar mass function with slope −2.8. Population III remnants do not satisfy any M_{BH}–σ relation either, as shown in Fig. 2 (lower left-hand panels).

When a halo enters the merger tree we assign seed MBHs by determining if the halo meets all the requirements described above (separately for each model). As we do not trace the metal enrichment of the intergalactic medium self-consistently, we consider here a sharp transition threshold, and assume that MBH seed formation ceases at $z \approx 15$ (cf. Volonteri et al. 2008).

3 TRACKING THE GROWTH OF MBHS

We follow the evolution of the MBH population resulting from the seed formation processes briefly outlined above in a ΛCDM Universe. We simulate the merger history of two sets of present-day haloes, one with mass $2 \times 10^{12}\,M_\odot$ mimicking the Milky Way (MW) and the other with mass $4 \times 10^{13}\,M_\odot$ mimicking a massive

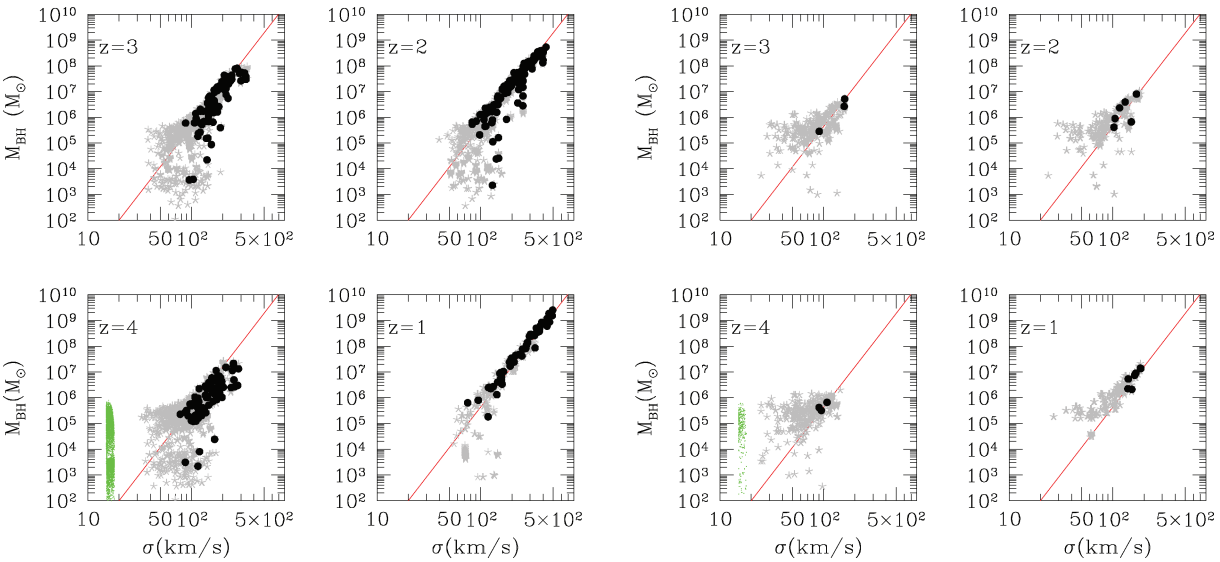

Figure 2. The M_{BH}–σ relation for MBHs at different redshifts along the merging history of a $4 \times 10^{13}\,M_\odot$ halo (ET, left-hand panels), and for a $2 \times 10^{12}\,M_\odot$ halo (MW, right-hand panels). The sample above comprises 20 realizations for each halo mass, and for each halo we include all the progenitors that exist at a given cosmic time. MBHs evolve from an initial population of seeds based on the model by Lodato & Natarajan (2006), with $Q_c = 2$ (the lack of any initial M_{BH}–σ correlation for seeds is clearly seen in the far left corner of the $z = 4$ panels, green points). Note that all the initial seeds in this model are overmassive compared to the local M_{BH}–σ relation. Grey points: all central MBHs in the progenitors of the galaxy at the specified redshift. Black points and triangles: all systems experiencing a MBH–MBH merger within the same redshift range (triangles indicate the less massive MBH of the pair). The velocity dispersion plotted is that of the merger remnant. Note the 'plume' of MBHs at $\sigma < 50\,\mathrm{km\,s^{-1}}$ that clearly persists even at $z = 2$ from the earliest epochs.

elliptical (ET), via a Monte Carlo algorithm based on the extended Press–Schechter formalism.

Here and throughout the paper, we use the velocity dispersion of the halo as a proxy for the central velocity dispersion σ (Ferrarese 2002; Pizzella et al. 2005). Every halo entering the merger tree is assigned a spin parameter drawn from the lognormal distribution in $\lambda_{\rm spin}$ found in numerical simulations, with mean $\bar{\lambda}_{\rm spin} = 0.05$ and standard deviation $\sigma_\lambda = 0.5$ (e.g. Warren et al. 1992; Cole & Lacey 1996; Bullock et al. 2001; van den Bosch et al. 2002). We assume that the spin parameter of a halo is not modified by its merger history, as no consensus exists on this issue at the present time.

We assume that, after seed formation ceases, the population of MBH progenitors evolves according to a 'merger driven scenario', as described in Volonteri et al. (2003) and Volonteri, Salvaterra & Haardt (2006). An accretion episode is assumed to occur as a consequence of every major merger (mass ratio larger than 1:10) event. Each MBH accretes an amount of mass, $\Delta M = 9 \times 10^7\,{\rm M}_\odot(\sigma/200\,{\rm km\,s^{-1}})^4$, that corresponds to 90 per cent of the $M_{\rm BH}$–σ_* relation of its host halo (Ferrarese 2002). This choice allows us to take into account the contribution of mergers. If a MBH increases its mass beyond the $M_{\rm BH}$–σ relation, we shut its growth. During this phase a MBH would be classified as an AGN. The rate at which mass is accreted scales with the Eddington rate for the MBH, and is based on the results of galaxy merger simulations, which also heuristically track accretion on to a central MBH (Di Matteo et al. 2005; Hopkins et al. 2005). We impose a lower limit to the Eddington ratio of $f_{\rm Edd} = 10^{-3}$. Accretion starts after a dynamical time-scale and lasts until the MBH has accreted ΔM. The lifetime of AGN therefore depends on how much mass it accretes in each episode,

$$t_{\rm AGN} = t_{\rm Edd}\, f_{\rm Edd} \frac{\epsilon}{1-\epsilon} \ln(M_{\rm fin}/M_{\rm BH}), \quad (4)$$

where $M_{\rm fin} = \min(M_{\rm BH} + \Delta M, M_{\rm BH}$–$\sigma)$; ϵ is the radiative efficiency (which depends with the MBH spin, $\langle\,\epsilon\rangle \approx 0.2$, assuming coherent accretion, Berti & Volonteri 2008) and $t_{\rm Edd} = 0.45$ Gyr. The farther away a MBH is from the $M_{\rm BH}$–σ, the longer it shines before accretion is shut when it reaches the $M_{\rm BH}$–σ limit.

In this scheme, we assume that MBHs accrete a gas mass that scales with the fifth power of the circular velocity (or equivalently σ) of the host halo. We do not assume any evolution of either slope or normalization of this scaling with redshift. Given this assumption, it is clearly not our goal to study the evolution of the slope and normalization of the observed $M_{\rm BH}$–σ relation or the scatter with redshift. We focus on analysing how MBH seeds, that do not initially satisfy any correlation with the host mass or velocity dispersion, migrate towards the observed correlation at $z = 0$ as a function of cosmic time. In this context, the exact scaling of the accreted mass does not affect our results, as long as accretion is merger driven and it establishes a clear correlation between hole and host.

In a hierarchical universe, where galaxies grow by mergers, MBH coalescences are a natural consequence, and we trace their contribution to the evolving MBH population (cf. Sesana, Volonteri & Haardt 2007 for details on the dynamical modelling). During the final phases of a MBH merger, emission of gravitational radiation drives the orbital decay of the binary. Recent numerical relativity simulations suggest that merging MBH binaries might be a subject to a large 'gravitational recoil': a general-relativistic effect due to the non-zero net linear momentum carried away by gravitational waves in the coalescence of two unequal MBHs (Fitchett 1983; Redmount & Rees 1989). Radiation recoil is a strong field effect that depends on the lack of symmetry in the system, and for merging MBHs with high spin in particular orbital configurations, the recoil velocity can be as high as a few thousands of kilometres per second. We include the effects of gravitational recoil by adopting the fitting formula proposed by Lousto & Zlochower (2009; see also Baker et al. 2008). MBHs that are displaced from galaxy centres by the gravitational recoil effect produce a population of *wandering* MBHs and AGNs as explored in earlier work (Volonteri & Perna 2005; Devecchi et al. 2009; Volonteri & Madau 2008).

4 TRACKING THE $M_{\rm BH}$–σ RELATION

We present the results of tracking the assembly history of MBHs in two classes of galaxies: (i) a dark matter halo with mass $2 \times 10^{12}\,{\rm M}_\odot$ that hosts a MW-type galaxy and (ii) a more massive dark matter halo, $4 \times 10^{13}\,{\rm M}_\odot$, that hosts a massive early type (ET) galaxy. The progenitors of the MBHs in each of these host haloes are tracked and plotted as measured at a given epoch. We analyse 20 realizations for each halo, to account for cosmic variance. Examples of growth histories are shown in Fig. 1, while statistical $M_{\rm BH}$–σ relations are shown in Figs 2 and 3 for the two seed models.

As outlined earlier, in propagating the seeds it is assumed that accretion episodes and therefore growth spurts are triggered only by major mergers. We find that in a merger-driven scenario for MBH growth the most biased galaxies at every epoch host the most massive MBHs that are most likely already sitting on the $M_{\rm BH}$–σ relation. Lower mass MBHs (below $10^6\,{\rm M}_\odot$) are instead off the relation at $z = 4$ and even at $z = 2$. These baseline results are independent of the seeding mechanism. In the 'heavy seeds' scenario, most of the MBH seeds start out *well above* the $z = 0$ $M_{\rm BH}$–σ, that is, they are 'overmassive' compared to the local relation. Seeds form only in haloes within a narrow range of velocity dispersion ($\sigma \simeq 15\,{\rm km\,s^{-1}}$, see equations 1 and 3, and Fig. 1). The MBH mass corresponding to $\sigma \simeq 15\,{\rm km\,s^{-1}}$, according to the local $M_{\rm BH}$–σ relation, would be $\sim 3 \times 10^3\,{\rm M}_\odot$. The mass function instead peaks at $10^5\,{\rm M}_\odot$ (Lodato & Natarajan 2007). As time elapses, all haloes are bound to grow in mass by mergers. The lowest mass haloes, though, experience mostly minor mergers, that do not trigger accretion episodes, and hence do not grow the MBH. The evolution of these systems can be described by a shift towards the right of the $M_{\rm BH}$–σ relation: σ increases, but $M_{\rm BH}$ stays roughly constant. Such systems are clearly seen at $z = 1$ in Fig. 2, with $M_{\rm BH} \sim 10^5\,{\rm M}_\odot$ and $\sigma < 100\,{\rm km\,s^{-1}}$. Effectively, for the lowest mass haloes growth of the galaxy and the central MBH are not coeval but rather sequential.

In the case of Population III seeds as well, there is initially no correlation between seed mass and halo mass or velocity dispersion. Here, we have assumed that the seeds form in the mass range $125 < M_{\rm BH} < 1000\,{\rm M}_\odot$. The initial $M_{\rm BH}$–σ relation would therefore appear as a horizontal line at $\sim 200\,{\rm M}_\odot$ (shown at the bottom of Fig. 3, $z = 4$ panels). In this case, MBHs migrate on to the $M_{\rm BH}$–σ always from *below*, as seeds are initially 'undermassive' compared to the local relation (Fig. 1, bottom panels). Underfed survivors of the seed epoch shift towards the right of the $M_{\rm BH}$–σ relation and lie in the lower left corner of Fig. 3, with $M_{\rm BH} \sim 10^2$–$10^3\,{\rm M}_\odot$ and $\sigma < 100\,{\rm km\,s^{-1}}$.

There appears to be a distinct difference between the journey of MBH seeds on to the $M_{\rm BH}$–σ relation predicted by the two seeding models considered here. The Population III seeds start life 'undermassive' lying initially below the local $M_{\rm BH}$–σ and they transit up to the relation by essentially growing the MBH without significantly altering σ. In contrast, the massive seeds start off above the local $M_{\rm BH}$–σ relation, and migrate on to it by initially growing

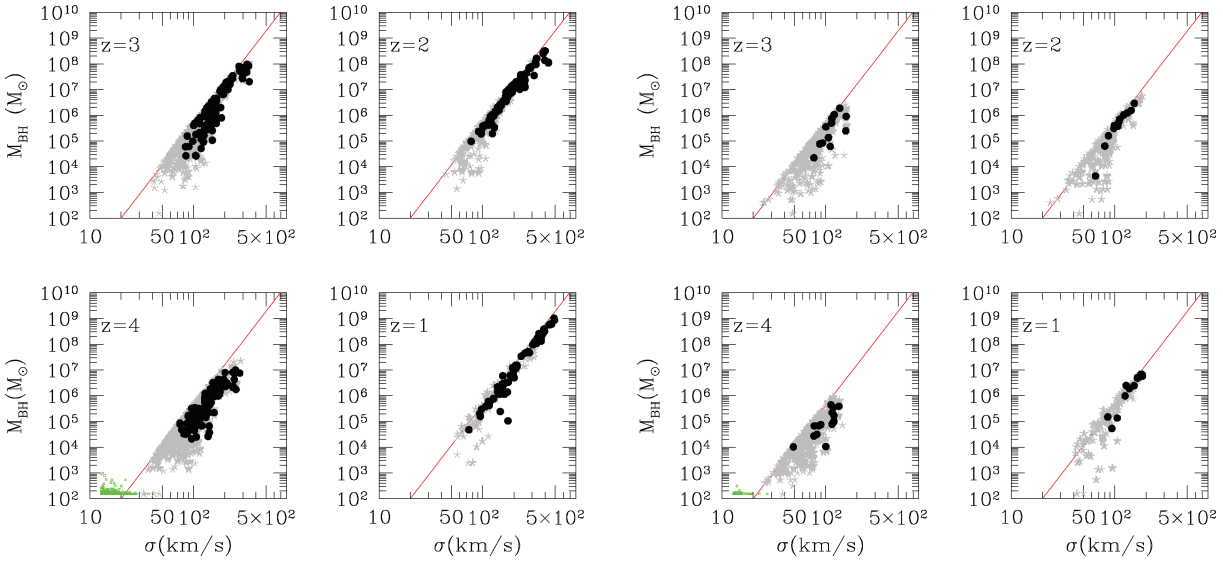

Figure 3. Same as Fig. 2, for Population III remnant seeds. The lack of an initial M_{BH}–σ correlation for these seeds is also evident here and is shown at the bottom of the $z = 4$ panels for the MW and ET halo realizations (green points). Note that the sharp difference in the assignment of the initial seed population $z = 15$ in the two models is evident even in the $z = 4$ panel.

σ, after which further major mergers trigger accretion episodes and therefore growth spurts for the MBHs. When MBHs are more massive than expected compared to the M_{BH}–σ relation, accretion is terminated very rapidly in our scheme (physically, we expect feedback to be responsible for shutting down accretion, see, e.g. Silk & Rees 1998; Fabian 2001).

4.1 What anchors the M_{BH}–σ relation?

It appears that major mergers that trigger accretion episodes are what set up the relation initially at high redshift. Our conclusions in this regard are in agreement with those reached by alternative arguments, for instance see Peng (2007) and Robertson et al. (2006). Biased peaks in the halo mass distribution, which are the sites for the formation of the largest galaxies, host the earliest massive MBHs that fall on the relation. Hence, the M_{BH}–σ correlation is established first for MBHs hosted in the largest haloes present at any time. MBHs in small galaxies lag behind, as their hosts are subject to little or no major merger activity. In many cases, the MBHs remain at the original seed mass for billions of years (e.g. see Fig. 2, the $z = 1$ panel). We find that these conclusions hold irrespective of our initial seeding mechanism and the relation tightens considerably from $z = 4$ to 1, especially for MBHs hosted in haloes with $\sigma > 100\,\mathrm{km\,s^{-1}}$. We find that if black hole seeds are massive, $\sim 10^5\,\mathrm{M}_\odot$, the low-mass end of the M_{BH}–σ flattens at low masses towards an asymptotic value, creating a characteristic 'plume'. This 'plume' consists of ungrown seeds, that merely continue to track the peak of the seed mass function at $M_{BH} \sim 10^5\,\mathrm{M}_\odot$ down to late times. For the Population III seed case, since the initial seed mass is very small, the plume of MBHs with $M_{BH} \sim 10^5$–$10^6\,\mathrm{M}_\odot$ in haloes with $\sigma \sim 40$–$50\,\mathrm{km\,s^{-1}}$ disappears.

5 OBSERVATIONAL CONSEQUENCES

We track MBH assembly histories with a view to understand two kinds of observations, observations of actively accreting MBHs as probed by flux limited AGN surveys and potential observations of gravitational waves emitted by merging MBHs. Note that in our model not every galaxy merger causes a merger of MBHs as one of the two galaxies might not be seeded. If the halo mass ratio is 1:10 or higher, every galaxy merger (where at least one of the galaxy hosts a MBH) triggers accretion and therefore such cases will be detected as an AGN. AGNs are therefore more common than MBH mergers, in our scheme.

5.1 Seed signatures: the AGN population

Since it is during accretion episodes that MBHs move on to the M_{BH}–σ relation, AGN are better tracers of the correlation itself, and worse tracers of the original seeds. Differences between seeding models appear only at the low-mass end. We predict the existence of many low-luminosity accretors with masses off the relation at $z = 4$ down to 3. These 'outliers' are mostly objects with $M_{BH} < 10^6\,\mathrm{M}_\odot$, making them rather faint sources. For instance, for an Eddington ratio of 0.1, this black hole mass corresponds to an X-ray luminosity in the 2–10 kev band of $7.8 \times 10^{42}\,\mathrm{erg\,s^{-1}}$ or B-band luminosity $1.5 \times 10^{43}\,\mathrm{erg\,s^{-1}}$. At $z = 3$, these luminosities correspond to fluxes of order a few times $10^{-16}\,\mathrm{erg\,s^{-1}\,cm^{-2}}$ (as a reference, the Chandra Deep Field North has a flux limit $3 \times 10^{-16}\,\mathrm{erg\,s^{-1}\,cm^{-2}}$).

The population of active MBHs shining above a flux limit $10^{-16}\,\mathrm{erg\,s^{-1}\,cm^{-2}}$ (bolometric) in the history of our ET galaxies is shown in Fig. 4. From Fig. 4, we note that the seed scenarios are less distinguishable for active MBHs than for the case of quiescent MBHs (Figs 2 and 3). The massive end of M-sigma, as traced by AGN, is well populated at $z = 4$ and 3 and its only at $z < 2$ that lower masses get on to the relation. The figure also shows that within the mass range probed by current flux-limited survey seed formation models are indistinguishable. The 'outliers' off the M_{BH}–σ, with $M_{BH} < 10^6\,\mathrm{M}_\odot$, are currently not easily observable, but future, planned X-ray missions with higher sensitivity might uncover this population.

Since MBHs move on to the M_{BH}–σ relation starting from the most massive systems at any time, the implication of our result is that flux limited AGN surveys tend to be biased towards finding MBHs that preferentially fall and anchor the M_{BH}–σ relation. Flux limited surveys indeed preferentially select the most massive

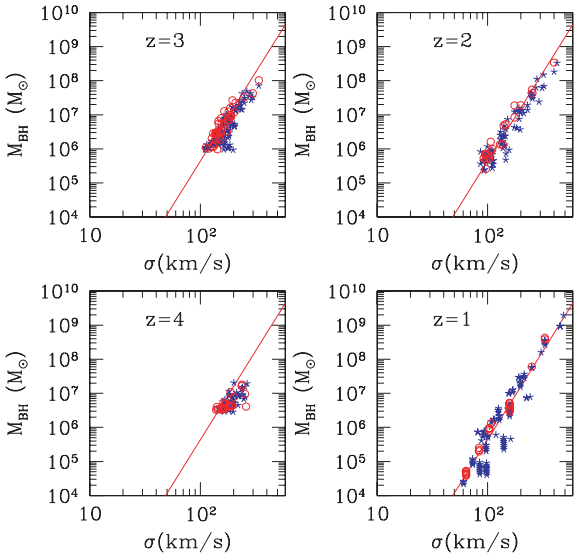

Figure 4. The M_{BH}–σ relation for active MBHs at different redshift slices in the ET progenitors. These MBHs would be observed as AGNs. We imposed a flux threshold, 10^{-16} erg s^{-1} cm^{-2} (bolometric). Stars: massive seeds based on the model by Lodato & Natarajan (2006), with $Q_c = 2$. Circles: seeds based on Population III star remnant models (Volonteri et al. 2003). The figure shows both central and satellite MBHs (satellite holes are shown at the σ of the host halo). The sample comprises all the progenitors of 20 $z = 0$ haloes.

accreting MBHs residing in the most massive galaxies (Lauer et al. 2007), assuming that MBHs accrete below the Eddington rate (e.g. Kelly, Vestergaard & Fan 2009).

5.2 Seed signatures: MBH mergers and gravitational waves

An alternative to AGN observations in electromagnetic bands is the detection of MBHs via gravitational radiation, that would be detectable by LISA. The merger rate of MBHs in our models and the detectability of binaries have been discussed in Sesana et al. (2007), where the impact of different 'seed' formation scenarios was taken into account.

Since the focus of this paper is high-redshift objects, we assume that merging is driven by dynamical friction, which has been shown to efficiently drive the MBHs in the central regions of the newly formed galaxy when the mass ratio of the satellite halo to the main halo is sufficiently large, $\geqslant$ 1:10 and galaxies are gas rich (Callegari et al. 2009). The available simulations (Escala et al. 2004; Dotti, Colpi & Haardt 2006; Mayer et al. 2007) show that the binary can shrink to about parsec or slightly subparsec scale by dynamical friction against gas.

We refer the reader to Sesana et al. (2007) and Sesana et al. (2005) for a detailed discussion of how we model the gravitational wave emission and the expected event rate. Detection of gravitational radiation provides accurate measurements of the mass of the components of MBH binaries prior to merger, and the mass of the single merger remnant. Additionally, the mass of 'single' MBHs can be determined by the inspiral of an extreme or intermediate mass-ratio compact object (EMRI/IMRI; Miller 2005). We will discuss EMRI/IMRI events in Section 5.3.

When we track the merging population, we find that MBH–MBH mergers also preferentially sample the region of space where MBHs lie on the M_{BH}–σ relation. This is once again a consequence of halo bias. Both formation models that we investigate in this paper require deep potential wells for gas retention and cooling as a prerequisite for MBH formation. Haloes where massive seeds can form are typically 3.5–4σ peaks of the density fluctuation field at $z > 15$, (the host haloes in the direct collapse model are slightly more biased than in the Population III remnant case). MBH seeding is therefore infrequent, MBHs are rare and as a consequence MBH–MBH mergers are events that typically involve only the most biased haloes at any time.

In typical mergers we find that the higher mass black hole in the binary tends to sit on or near the expected M_{BH}–σ relation for the host (which corresponds to the newly formed galaxy after the merger). The mass of the secondary generally provides clues to the dynamics of the merger, rather than to the M_{BH}–σ relation, since at the time of the merger any information that we can gather on the host (via electromagnetic observations) will not provide details on the two original galaxies. For instance, the mass ratio of the merging MBHs encodes how efficiently minor mergers can deliver MBHs to the centre of a galaxy in order to form a bound binary.

5.3 Hidden black holes

Our key finding is the prediction of the existence of a large population of hidden (as in undetectable as AGN or as merging BHs via gravitational radiation) MBHs at all redshifts. There are two main contributors to the population of hidden MBHs: MBHs in the *nuclei* of low-mass galaxies ($\sigma \sim$ 20–50 km s^{-1}), and satellite/wandering MBHs. 'Hidden' nuclear MBHs have not experienced appreciable growth in mass and formed in low-mass haloes with quiet merging histories. A potential observational signature of the 'heavy seed' scenario is the existence of a 'plume' of overmassive MBHs in the *nuclei* of haloes with $\sigma \sim$ 20–50 km s^{-1}. The only way to detect MBHs in the plume would be as IMRI/EMRI (intermediate or extreme mass-ratio inspiral) events or via measurement of stellar velocity dispersions and modelling as in the local universe (e.g. Magorrian et al. 1998). Approaching $z = 0$, the underfed part of this population likely merges into more massive galaxies.

Satellite and wandering MBHs would instead be off-centre systems, orbiting in the potential of comparatively massive hosts. Semantically, we distinguish here between MBHs that are infalling into a galaxy for the very first time, following a galaxy merger (satellite MBHs) and those that are merely displaced from the centre due to gravitational recoil (wandering MBHs). Some of the *satellite* MBHs will merge with the central MBH in the primary galaxy, and such merging does not significantly alter the position of the already massive primary hole which sits on the M_{BH}–σ relation to start with.

The MBH population in our series of simulations of the massive ET halo is shown in Fig. 5, for $z = 1$. Here, we dissect the MBH population into its components. Satellite/wandering MBHs are found *below* the M_{BH}–σ correlation as expected (shown as open circles, at the σ of the host halo). Luminous AGNs are preferentially found on the M_{BH}–σ relation (squares). We note the existence of a subpopulation of satellite AGNs, that is, satellite MBHs which are actively accreting. For every pair of coalescing MBHs (triangles), one typically sits on the M_{BH}–σ relation, while the companion tends to be less massive, hence, when they merge, the remnant finds itself in the right spot on the M_{BH}–σ relation (solid circles).

6 CONCLUSIONS AND DISCUSSION

In this paper, we have investigated how the M_{BH}–σ relation is populated at the earliest times for models with physically motivated

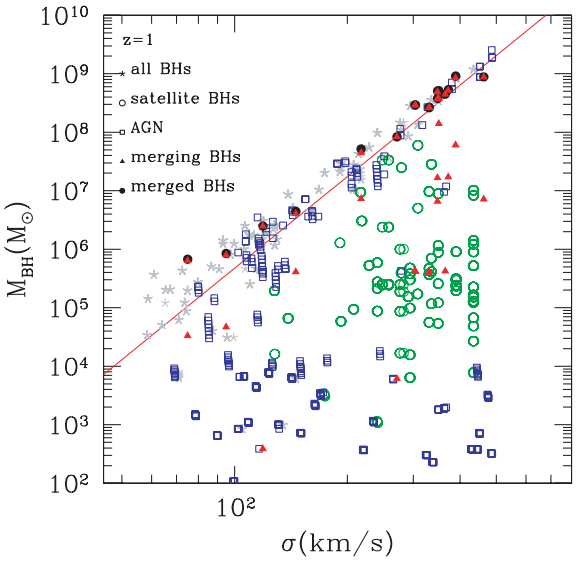

Figure 5. Dissecting the MBH population at $z = 1$: MBH population in our 20 ET haloes at $z = 1$ (integrating over seven time-steps, for a total of 0.2 Gyr). Here, all MBHs evolve from the massive seeding model of Lodato & Natarajan (2006), with $Q_c = 2$. Stars: all nuclear MBHs. Empty circles: satellite/wandering MBHs. Squares: AGNs. Triangles: merging MBHs. Solid circles: merger remnants. AGN and merging MBHS represent the detectable systems. Note that accreting MBHs (powering AGNs) grow notably in mass during the seven time-steps and progress towards the local $M_{\rm BH}$–σ relation.

initial black hole seeds. Starting with ab initio MBH seed mass functions computed in the context of 'heavy seeds' (direct formation of central objects from the collapse of pre-galactic discs in high-redshift haloes) or 'light seeds' (Population III remnants) we follow the assembly history to late times using a Monte Carlo merger tree approach. The initial seeding does not set up the $M_{\rm BH}$–σ relation. In our calculation of the evolution and build-up of mass, we assume a simple prescription for determining the precise mass gain by the MBH during a merger. Motivated by the phenomenological scaling of $M_{\rm BH} \propto \sigma^{4-5}$, we assume that this proportionality carries over to the gas mass accreted in each step. This simple assumption allows us to meet a number of observational constraints, including the luminosity function of quasars and the mass density in MBHs at $z = 0$ (Volonteri et al. 2008).

Here follows a summary of our results.

(i) We find that the $M_{\rm BH}$–σ relation can be established early due to accretion episodes associated with major mergers even though the original MBH seeds themselves do not satisfy this relation.

(ii) At the high-mass end ($M_{\rm BH} > 10^6\,{\rm M}_\odot$), the relation is anchored early, and low-mass MBHs slowly migrate on to it as hierarchical merging proceeds.

(iii) Among active accretors, the most massive MBHs ($M_{\rm BH} > 10^6\,{\rm M}_\odot$) sit on or around the $M_{\rm BH}$–σ relation at all epochs and consequently flux limited AGN surveys are biased to preferentially detect this population.

(iv) Similarly, we find that LISA is also likely to be biased towards detecting black holes that preferentially inhabit the $M_{\rm BH}$–σ relation. This bias is due to major mergers being more common at high redshift for the most massive, biased, galaxies.

Since we assume a priori that the accreted mass during a major merger event scales as the fifth power of the velocity dispersion, we inevitably recover the observed $z = 0$ slope. Our current formalism therefore does not equip us strictly speaking to study the evolution of the relation or the scatter with redshift. However, the exact scaling of the accreted mass does not affect our results, as long as accretion is merger-driven and it establishes a clear correlation between hole and host. To push this scenario further, we have implemented a model where the $M_{\rm BH}$–σ correlation evolves with redshift as proposed by Woo et al. (2008), based on observations of $z \sim 0.5$ AGN. We have simply assigned to MBHs hosted in galaxies experiencing a major merger a mass corresponding to the extrapolation at all redshifts of the scaling suggested by Woo et al.: at fixed velocity dispersion $\log M_{\rm BH}(z) - \log M_{\rm BH}(0) = 3.1\,\log(1+z) + 0.05$. This is the final mass that a MBH would have at the end of the accretion episode. This relation has been proposed for $z \sim 0.5$ objects. We applied the same scaling all the way to high redshift, further imposing that the MBH mass is not larger than the galaxy mass. Implementing such rapid evolution, we find overproduces the local MBH mass density and overestimates the luminosity function of quasars, while the main conclusions of the present paper are otherwise unchanged.

As a further check of our result that the establishment of the $M_{\rm BH}$–σ is a function of the halo bias and hierarchy, we have tested a model where the accreted mass does not correlate with the velocity dispersion at all. For this scenario, we assume a prescription for black hole growth, simply that MBHs *double* in mass at every major merger with no implemented self-regulation prescription. This model allows us to explore the effect of the number of major mergers on MBH growth (i.e. the connection with the cosmic bias). Although the resulting $M_{\rm BH}$–σ has a larger scatter at all redshifts and the local MBH mass density and luminosity function of quasars are overestimated; we still recover a correlation between $M_{\rm BH}$ and σ, in the sense that the most massive galaxies do tend to host the most massive holes. Since in this case there is no correlation between accreted mass and halo properties, this exercise confirms that the existence of this correlation is a pure reflection of the merger history: the most massive haloes experience a larger number of major mergers over their lifetime, hence their MBHs are the first to grow, and become the largest. The slope of the $M_{\rm BH}$–σ correlation is however much flatter than the local empirical correlation ranging from 2 (for massive seeds) to 3.4 (for Population III seeds) instead of 4–5. We note here that the scatter obtained in the $M_{\rm BH}$–σ at $z = 0$ in all the models studied here reflects both the seeding mechanism (the spread in seed masses) and the prescription used for self-regulation.

One of our key predictions is the existence of a large population of low-mass 'hidden' MBHs at high redshift which are undetectable by flux limited AGN surveys and at merger by LISA, that at later times likely end up as wandering MBHs. This population of low-mass black holes is outliers at all epochs on the $M_{\rm BH}$–σ relation. Outliers can be detected as IMRI/EMRI gravitational waves events or via stellar dynamical $M_{\rm BH}$ measurements in low–mass galaxies. We find that nuclear MBHs with masses in excess of $M_{\rm BH} \sim 10^6\,{\rm M}_\odot$ preferentially lie on the $M_{\rm BH}$–σ correlation. More accurate measurements of MBH masses below $M_{\rm BH} \sim 10^6\,{\rm M}_\odot$ will enable us to use the measured $z = 0$ relation to constrain seeding models at high redshift since cosmic evolution does not appear to smear out this imprint of the initial conditions. The scatter in the observed $M_{\rm BH}$–σ relation might also provide insights into the initial seeding mechanism. Since Population III remnants do not appear to be efficient seeds (Alvarez, Wise & Abel 2009), other channels like the one proposed by Lodato & Natarajan, for instance, are clearly needed to make massive seeds. It appears that the local relation might indeed hold clues to initial seeding mechanism.

ACKNOWLEDGMENTS

PN would like to thank the Radcliffe Institute for Advanced Study and the Center for Astrophysics (CfA) for providing an intellectually stimulating atmosphere that enabled this work. Support for this work was provided by NASA grant NNX07AH22G and SAO Awards SAO-G07-8138 C and TM9-0006X (M.V.).

REFERENCES

Alvarez M.-A., Wise J.-H., Abel T., 2009, ApJ, 701, L133
Baker J. G., Boggs W. D., Centrella J., Kelly B. J., McWilliams S. T., Miller M. C., van Meter J. R., 2008, ApJ, 682, L29
Begelman M. C., Volonteri M., Rees M. J., 2006, MNRAS, 370, 289
Berti E., Volonteri M., 2008, ApJ, 684, 822
Bullock J. S., Dekel A., Kolatt T. S., Kravtsov A. V., Klypin A. A., Porciani C., Primack J. R., 2001, ApJ, 555, 240
Callegari S., Mayer L., Kazantzidis S., Colpi M., Governato F., Quinn T., Wadsley J., 2009, ApJ, 696, L89
Carr B. J., Bond J. R., Arnett W. D., 1984, ApJ, 277, 445
Cole S., Lacey C., 1996, MNRAS, 281, 716
Devecchi B., Rasia E., Dotti M., Volonteri M., Colpi M., 2009, MNRAS, 394, 633
Di Matteo T., Springel V., Hernquist L., 2005, Nature, 433, 604
Dotti M., Colpi M., Haardt F., 2006, MNRAS, 367, 103
Escala A., Larson R. B., Coppi P. S., Mardones D., 2004, ApJ, 607, 765
Fabian A. C., 2001, X-ray Astronomy: Stellar Endpoints AGN, and the Diffuse X-ray Background, 599, 93
Ferrarese L., 2002, ApJ, 578, 90
Ferrarese L., Merritt D., 2000, ApJ, 539, 9
Fitchett M. J., 1983, MNRAS, 203, 1049
Fryer C. L., Woosley S. E., Heger A., 2001, ApJ, 550, 372
Gebhardt K. et al., 2000, AJ, 119, 1157
Gültekin K. et al., 2009, ApJ, 698, 198
Haehnelt M. G., Natarajan P., Rees M. J., 1998, MNRAS, 300, 817
Haiman Z., Loeb A., 1998, ApJ, 503, 505
Háring N., Rix H.-W., 2004, ApJ, 604, L89
Hopkins P.-F., Hernquist L., Cox T.-J., Di Matteo T., Robertson B., Springel V., 2005, ApJ, 630, 716
Hopkins P.-F., Bundy K., Hernquist L., Ellis R.-S., 2007a, ApJ, 659, 976
Hopkins P.-F., Hernquist L., Cox T.-J., Robertson B., Krause E., 2007b, ApJ, 669, 67
Kauffmann G., Haehnelt M., 2000, MNRAS, 311, 576
Kauffmann G., Haehnelt M. G., 2002, MNRAS, 332, 529
Kelly B. C., Vestergaard M., Fan X., 2009, ApJ, 692, 1388
King A., 2003, ApJ, 596, L27
Koushiappas S. M., Bullock J. S., Dekel A., 2004, MNRAS, 354, 292
Lacey C., Cole S., 1993, MNRAS, 262, 627
Lauer T. R., Tremaine S., Richstone D., Faber S. M., 2007, ApJ, 670, 249
Lodato G., Natarajan P., 2006, MNRAS, 371, 1813
Lodato G., Natarajan P., 2007, MNRAS, 377, L64
Lousto C. O., Zlochower Y., 2009, Phys. Rev. D, 79, 064018
Madau P., Rees M. J., 2001, ApJ, 551, L27
Magorrian J. et al., 1998, AJ, 115, 2285
Marconi A., Hunt L. K., 2003, ApJ, 589, L21
Mayer L., Kazantzidis S., Madau P., Colpi M., Quinn T., Wadsley J., 2007, Sci, 316, 1874
Miller M. C., 2005, ApJ, 618, 426
Natarajan P., Treister E., 2009, MNRAS, 393, 838
Page L. et al., 2003, ApJS, 148, 233
Peng C. Y., 2007, ApJ, 671, 1098
Pizzella A., Corsini E. M., Dalla Bontà E., Sarzi M., Coccato L., Bertola F., 2005, ApJ, 631, 785
Redmount I. H., Rees M. J., 1989, Comments Astrophy., 14, 165
Rice W. K. M., Lodato G., Armitage P. J., 2005, MNRAS, 364, L56
Robertson B., Hernquist L., Cox T.-J., Di Matteo T., Hopkins P.-F., Martini P., Springel V., 2006, ApJ, 641, 90
Sesana A., Haardt F., Madau P., Volonteri M., 2005, ApJ, 623, 23
Sesana A., Volonteri M., Haardt F., 2007, MNRAS, 377, 1711
Silk J., Rees M. J., 1998, A&A, 331, L1
Spergel D. N. et al., 2003, ApJS, 148, 175
Steed A., Weinberg D. H., 2004, Multiwavelength AGN Surveys, 401
Thompson T. A., Quataert E., Murray N., 2005, ApJ, 630, 167
Tremaine S. et al., 2002, ApJ, 574, 740
van den Bosch F. C., Abel T., Croft R. A. C., Hernquist L., White S. D. M., 2002, ApJ, 576, 21
Volonteri M. F., Madau P., 2008, ApJ, 687, L57
Volonteri M., Perna R., 2005, MNRAS, 358, 913
Volonteri M., Rees M. J., 2006, ApJ, 650, 669
Volonteri M., Haardt F., Madau P., 2003, ApJ, 582, 559
Volonteri M., Salvaterra R., Haardt F., 2006, MNRAS, 373, 121
Volonteri M., Lodato G., Natarajan P., 2008, MNRAS, 383, 1079
Warren M. S., Quinn P. J., Salmon J. K., Zurek W. H., 1992, ApJ, 399, 405
Woo J.-H., Treu T., Malkan M. A., Blandford R. D., 2008, ApJ, 681, 925
Wyithe J. S. B., Loeb A., 2002, ApJ, 581, 886

This paper has been typeset from a TEX/LATEX file prepared by the author.